Subscriber access provided by ISTANBUL TEKNIK UNIV

Article

Vibrational Recognition of Adsorption Sites for CO on Platinum and Platinum–Ruthenium Surfaces

Ismaila Dabo, Andrzej Wieckowski, and Nicola Marzari

J. Am. Chem. Soc., **2007**, 129 (36), 11045-11052• DOI: 10.1021/ja067944u • Publication Date (Web): 17 August 2007

Downloaded from http://pubs.acs.org on February 14, 2009

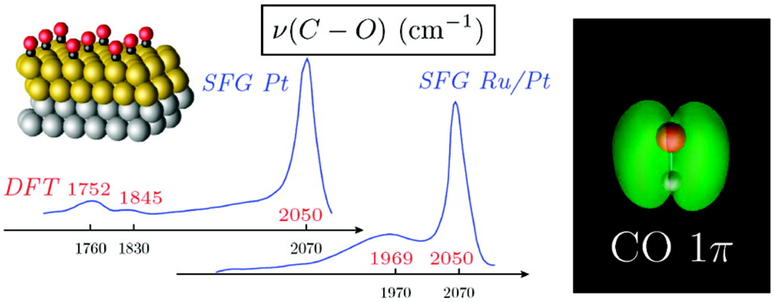

More About This Article

Additional resources and features associated with this article are available within the HTML version:

- Supporting Information
- Links to the 4 articles that cite this article, as of the time of this article download
- Access to high resolution figures
- Links to articles and content related to this article
- Copyright permission to reproduce figures and/or text from this article

View the Full Text HTML

Journal of the American Chemical Society is published by the American Chemical Society. 1155 Sixteenth Street N.W., Washington, DC 20036

J|A|C|S
ARTICLES

Published on Web 08/17/2007

Vibrational Recognition of Adsorption Sites for CO on Platinum and Platinum−Ruthenium Surfaces

Ismaila Dabo,[*,†] Andrzej Wieckowski,[‡] and Nicola Marzari[†]

Contribution from the Department of Materials Science and Engineering, Massachusetts Institute of Technology, 77 Massachusetts Avenue, Cambridge, Massachusetts 02139, and Department of Chemistry, University of Illinois at Urbana-Champaign, 600 South Mathews Avenue, Urbana, Illinois, 61801

Received November 7, 2006; E-mail: dabo_is@mit.edu

Abstract: We have studied the vibrational properties of CO adsorbed on platinum and platinum−ruthenium surfaces using density-functional perturbation theory within the Perdew−Burke−Ernzerhof generalized-gradient approximation. The calculated C−O stretching frequencies are found to be in excellent agreement with spectroscopic measurements. The frequency shifts that take place when the surface is covered with ruthenium monolayers are also correctly predicted. This agreement for both shifts and absolute vibrational frequencies is made more remarkable by the frequent failure of local and semilocal exchange-correlation functionals in predicting the stability of the different adsorption sites for CO on transition metal surfaces. We have investigated the chemical origin of the C−O frequency shifts introducing an orbital-resolved analysis of the force and frequency density of states, and assessed the effect of donation and backdonation on the CO vibrational frequency using a GGA + molecular U approach. These findings rationalize and establish the accuracy of density-functional calculations in predicting absolute vibrational frequencies, notwithstanding the failure in determining relative adsorption energies, in the strong chemisorption regime.

Introduction

Fuel cells are energy conversion systems of potentially high environmental benefit[1] that provide electricity and heat by catalytic conversion of a fuel, such as hydrogen or methanol. Despite their advantages, several technological obstacles have hindered the deployment of fuel-cell systems. For low-temperature fuel cells that use platinum as electrode material, one major limitation is CO poisoning, whereby CO occupies active sites on the platinum catalyst and prevents fuel oxidation.[2] Typically, in polymer electrolyte membrane fuel cells (PEMFCs), CO concentrations must be brought below 10−50 ppm to maintain an acceptable catalytic performance. For comparison, CO concentrations are generally on the order of thousands of ppm in reformed hydrogen fuels.[3] CO poisoning is even more problematic for direct methanol fuel cells (DMFCs) since CO is always present in critical amounts as an intermediate in methanol oxidation.[4]

Ruthenium islands on platinum catalysts have been shown to considerably attenuate CO poisoning,[5,6] although the microscopic details of this phenomenon are not completely understood. Two main mechanisms have been proposed to explain this improved tolerance to CO. Within the bifunctional-mechanism model, adsorbed OH species generated by water dissociation at the platinum/ruthenium edge promote the oxidation of CO (*the promotion effect*).[4,6−9] According to an alternative view, ruthenium modifies the electronic structure of neighboring platinum atoms, reducing their affinity for CO (*the ligand/intrinsic effect*).[4,9] To investigate further these mechanisms of central interest to fuel-cell technology, it is necessary to elucidate the nature of the chemical interaction between CO and bimetallic surfaces.

In most cases, density-functional theory provides a reliable description of molecular adsorption and dissociation on transition metals.[10−15] However, CO adsorption on transition metal surfaces is unexpectedly problematic. Indeed, at low CO

[†] Massachusetts Institute of Technology.

[‡] University of Illinois at Urbana-Champaign.

(1) Tester, J. W.; Drake, E. M.; Driscoll, M. J.; Golay, M. W.; Peters, W. A. *Sustainable Energy*; MIT Press, 2005.

(2) Larminie, J.; Dicks, A. *Fuel Cell Systems Explained*, 2nd ed.; Wiley-VCH: 2003.

(3) Vielstich, W.; Lamm, A.; Gasteiger, H. *Handbook of Fuel Cells: Fundamentals, Technology, Applications*; Wiley-VCH: 2003. Brandon, N. P.; Thompsett, D. *Fuel Cells Compendium*; Elsevier: 2005.

(4) Hoogers, G. *Fuel Cell Technology Handbook*; CRC Press: 2003.

(5) Cramm, S.; Friedrich, K. A.; Geyzers, K. P.; Stimming, U.; Vogel, R. *Fresenius' Journal Of Analytical Chemistry* **1997**, *358* (1−2), 189−192.

(6) Herrero, E.; Feliu, J. M.; Wieckowski, A. *Langmuir* **1999**, *15* (15), 4944−4948. Crown, A.; Johnston, C.; Wieckowski, A. *Surf. Sci.* **2002**, *506* (1−2), L268−L274.

(7) Tong, Y. Y.; Kim, H. S.; Babu, P. K.; Waszczuk, P.; Wieckowski, A.; Oldfield, E. *J. Am. Chem. Soc.* **2002**, *124* (3), 468−473.

(8) Maillard, F.; Lu, G.-Q.; Wieckowski, A.; Stimming, U. *J. Phys. Chem. B* **2005**, *109* (34), 16230−16243.

(9) Liu, P.; Logadottir, A.; Nørskov, J. K. *Electrochim. Acta* **2003**, *48* (25−26), 3731−3742.

(10) Hammer, B.; Morikawa, Y.; Nørskov, J. K. *Phys. Rev. Lett.* **1996**, *76* (12), 2141−2144.

(11) Hammer, B.; Nørskov, J. K. *Nature* **1995**, *376* (6537), 238−240.

(12) Nørskov, J. K.; Bligaard, T.; Logadottir, A.; Bahn, S.; Hansen, L. B.; Bollinger, M.; Bengaard, H.; Hammer, B.; Sljivancanin, Z.; Mavrikakis, M.; Xu, Y.; Dahl, S.; Jacobsen, C. J. H. *J. Catal.* **2002**, *209* (2), 275−278.

(13) Greeley, J.; Mavrikakis, M. *Nat. Mater.* **2004**, *3* (11), 810−815.

(14) Reuter, K.; Frenkel, D.; Scheffler, M. *Phys. Rev. Lett.* **2004**, *93*, 116105−116108.

(15) Hammer, B.; Hansen, L. B.; Nørskov, J. K. *Phys. Rev. B* **1999**, *59* (11), 7413−7421.

10.1021/ja067944u CCC: $37.00 © 2007 American Chemical Society

coverage, local and generalized-gradient density-functional calculations predict CO adsorption on Pt(111) to take place at the fcc site, contradicting low-temperature experiments, which unambiguously indicate atop adsorption. This well-known qualitative discrepancy (the "CO/Pt(111) puzzle")[16] precludes an accurate description of important phenomena, such as the surface diffusion of CO adsorbates and the thermal population of CO adsorption sites. Similar qualitative errors have been reported for CO adsorbed on rhodium and copper surfaces,[16−18] and a wide body of literature exists on the subject.[19−30]

In this work, we highlight and rationalize the accuracy of density-functional calculations in predicting the stretching frequencies of CO adsorbed on platinum and platinum−ruthenium surfaces, notwithstanding the failure in predicting the most stable adsorption site. We first present density-functional theory and density-functional perturbation theory results for the energetic, structural, and vibrational properties of adsorbed CO. Second, we introduce a novel orbital-resolved force analysis to clarify the electronic origins of the C−O frequency shifts as a function of the adsorption site. Last, we rationalize the accuracy of the stretching-frequency predictions by analyzing the influence of donation and backdonation using a GGA + molecular U model recently introduced by Kresse, Gil, and Sautet.[19]

Table 1. Adsorption Energies, Structural Properties, and Vibrational Frequencies Calculated Using Density-Functional Theory and Density-Functional Perturbation Theory for CO Adsorbed on Clean Pt(111) Surfaces[a]

site	atop	bridge	hcp	fcc
slab	4 ML Pt	4 ML Pt	4 ML Pt	4 ML Pt
E_{ads} (eV)	1.61 (1.30)[b]	1.71	1.72	1.74
d(C−O) (Å)	1.153	1.177	1.188	1.189
	(1.15 ± 0.05)[c]	(1.15 ± 0.05)[c]		
d(M−C) (Å)	1.864	2.029	2.116	2.121
	(1.85 ± 0.1)[c]	(2.08 ± 0.07)[c]		
h(C) (Å)	2.017	1.543	1.380	1.373
θ(CO) (deg)	1.4	1.4	0.5	0.4
ν(C−O) (cm^{-1})	2050	1845	1752	1743
	(2070)[d]	(1830)[d]	(1760)[d]	(1760)[d]
ν(M−C) (cm^{-1})	584	413	358	344
	(470)[e]	(380)[e]		
bending modes (cm^{-1})	392	393	329	328
	386	346	315	300
other modes (cm^{-1})	0 to 230	0 to 231	0 to 196	0 to 186

[a] h(C) denotes the distance from C to the first surface layer, and θ(CO) denotes the tilt angle of CO. [b] ref 35. [c] ref 36. [d] ref 37. [e] ref 38.

Theoretical Basis

The (111) transition metal surface is modeled using a periodically repeated slab composed of four layers, each layer containing four atoms per supercell. A $\sqrt{3} \times 2$ adsorption structure corresponding to a coverage of $^1/_4$ of the monolayer (ML) is adopted for the CO overlayer. Atomic cores are represented by ultrasoft pseudopotentials[31] (cf. Supporting Information). The exchange-correlation energy is calculated within the Perdew−Burke−Ernzerhof generalized-gradient approximation (PBE-GGA).[32] The size of the vacuum region separating the periodic slabs is ~13 Å. We use a shifted 4 × 4 × 1 mesh with cold-smearing occupations[33] (smearing temperature of 0.4 eV) to sample the Brillouin zone. Energy cutoffs of 24 and 192 Ry are applied to the plane-wave expansions of the wavefunctions and charge density, respectively. As discussed in ref 16, the system is not spin-polarized. Using the above slab thickness and calculation parameters, we verify that adsorption energies are converged within less than 10 meV and that atomic forces are converged within a few meV/Å.

The bond length and stretching frequency of CO in the gas phase are calculated to be 1.140 Å and 2140 cm^{-1} (experimental values are 1.128 Å and 2170 cm^{-1}). The PBE-GGA lattice parameter and bulk modulus of platinum are 3.993 Å and 2.36 Mbar, in good agreement with experimental values of 3.923 Å and 2.30 Mbar.[34] All our calculations use fully relaxed configurations.

Results

We report the results of our density-functional calculations in Tables 1 and 2. For platinum surfaces, the calculated atop binding energy $E_{\mathrm{ads}}(\mathrm{atop}) = 1.61$ eV is consistent with that reported in ref 39 (1.55 eV in the same adsorption structure). As a matter of comparison, the experimental heat of adsorption at $^1/_4$ ML CO is 1.30 eV. The relative adsorption energy $E_{\mathrm{ads}}(\mathrm{atop}) - E_{\mathrm{ads}}(\mathrm{fcc})$ is calculated to be −0.13 eV, in accordance with the gradient-corrected relative adsorption energies (ranging from −0.10 to −0.25 eV) reported in ref 16. As expected, our density-functional calculations favor CO adsorption at the threefold fcc and hcp sites for platinum and platinum−ruthenium surfaces, confirming the aforementioned disagreement with experiments. (Note that bridge adsorption of CO on platinum−ruthenium surfaces is predicted to be energetically unstable.) Despite this noteworthy failure, the bond length d(C−O) is calculated to be 1.153 Å at the atop site and 1.177 Å at the bridge site on platinum, in good agreement with experimental bond lengths (1.15 ± 0.05 Å at both the atop and fcc sites). Similarly, the distance d(Pt−C) from the carbon to its nearest platinum neighbor, calculated to be 1.864 Å at the atop site and 2.029 Å at the fcc site, is always within experimental error (experimental bond lengths are 1.85 ± 0.1 Å and 2.08 ± 0.07 Å at the atop and fcc sites, respectively). Note that both bond lengths increase with coordination.

The full phonon spectra for CO adsorbed at the atop, bridge, hcp, and fcc sites on platinum and platinum−ruthenium surfaces

---

(16) Feibelman, P. J.; Hammer, B.; Nørskov, J. K.; Wagner, F.; Scheffler, M.; Stumpf, R.; Watwe, R.; Dumesic, J. *J. Phys. Chem. B* **2001**, *105* (18), 4018−4025.
(17) Gajdoš, M.; Hafner, J. *Surf. Sci.* **2005**, *590* (2−3), 117−126.
(18) Köhler, L.; Kresse, G. *Phys. Rev. B* **2004**, *70*, 165405−165013.
(19) Kresse, G.; Gil, A.; Sautet, P. *Phys. Rev. B* **2003**, *68*, 73401−73404.
(20) Grinberg, I.; Yourdshahyan, Y.; Rappe, A. M. *J. Chem. Phys.* **2002**, *117* (5), 2264−2270.
(21) Mason, S. E.; Grinberg, I.; Rappe, A. M. *Phys. Rev. B* **2004**, *69*, 161401−161404.
(22) Grönbeck, H. *Surf. Sci.* **2004**, *559* (2−3), 214−222.
(23) Doll, K. *Surf. Sci.* **2004**, *573* (3), 464−473.
(24) Neef, M.; Doll, K. *Surf. Sci.* **2006**, *600* (5), 1085−1092.
(25) Wu, X.; Vargas, M. C.; Nayak, S.; Lotrich, V.; Scoles, G. *J. Chem. Phys.* **2001**, *115* (19), 8748−8757.
(26) Orita, H.; Itoh, N.; Inada, Y. *Chem. Phys. Lett.* **2004**, *384* (4−6), 271−276.
(27) Olsen, R. A.; Philipsen, P. H. T.; Baerends, E. J. *J. Chem. Phys.* **2003**, *119* (8), 4522−4528.
(28) Birgersson, M.; Almbladh, C.-O.; Borg, M.; Andersen, J. N. *Phys. Rev. B* **2003**, *67*, 45402−45413.
(29) Greeley, J.; Gokhale, A. A.; Kreuser, J.; Dumesic, J. A.; Topsøe, H.; Topsøe, N. Y.; Mavrikakis, M. *J. Catal.* **2003**, *213* (1), 63−72.
(30) Mavrikakis, M.; Rempel, J.; Greeley, J.; Hansen, L. B.; Nørskov, J. K. *J. Chem. Phys.* **2002**, *117* (14), 6737−6744.
(31) Vanderbilt, D. *Phys. Rev. B* **1990**, *41* (11), 7892−7895.
(32) Perdew, J. P.; Burke, K.; Ernzerhof, M. *Phys. Rev. Lett.* **1996**, *77* (18), 3865−3868.
(33) Marzari, N. PhD Dissertation, University Of Cambridge, 1996.
(34) *CRC Handbook of Chemistry and Physics*; CRC Press: 2004.

Table 2. Adsorption Energies, Structural Properties, and Vibrational Frequencies Calculated Using Density-Functional Theory and Density-Functional Perturbation Theory for CO Adsorbed on Ruthenium-Covered Pt(111) Surfaces[a]

site	atop	hcp	fcc	atop	hcp	fcc
slab	1 ML Ru/ 3 ML Pt	1 ML Ru/ 3 ML Pt	1 ML Ru/ 3 ML Pt	2 ML Ru/ 2 ML Pt	2 ML Ru/ 2 ML Pt	2 ML Ru/ 2 ML Pt
E_{ads} (eV)	2.24	2.27	2.15	1.96	2.05	1.88
d(C−O) (Å)	1.161	1.196	1.192	1.161	1.201	1.190
d(M−C) (Å)	1.892	2.132	2.104	1.922	2.122	2.111
h(C) (Å)	2.014	1.375	1.412	1.970	1.318	1.437
θ(CO) (deg)	3.3	0.9	2.6	4.1	0.6	1.44
ν(C−O) (cm^{-1})	1979 (1970)[b]	1702	1724	1969 (1970)[b]	1666	1739
ν(M−C) (cm^{-1})	510	356	358	482	355	351
bending modes (cm^{-1})	412	258	221	396	315	251
	409	247	215	389	301	231
other modes (cm^{-1})	0 to 208	0 to 205	0 to 201	0 to 265	0 to 254	0 to 226

[a] h(C) denotes the distance from C to the first surface layer, and θ(CO) denotes the tilt angle of CO. Note that bridge adsorption of CO on ruthenium-covered Pt(111) is unstable. [b] ref 37.

are calculated using density-functional perturbation theory (DFPT).[40] Within this approach, the full dynamical matrix of the system is computed exactly by solving the self-consistent linear-response problem describing the electron response to atomic perturbations corresponding to arbitrary wavelengths. The DFPT spectra reported in Tables 1 and 2 exhibit some common and expected features. The highest vibrational frequency in the range [1700 cm^{-1}, 2100 cm^{-1}] corresponds to the localized C−O stretching mode. The second highest frequency ν(M−C) in the range [300 cm^{-1}, 600 cm^{-1}] is related to the stretching of the metal−carbon bond. This mode is followed by two CO bending modes with frequencies lying 20−200 cm^{-1} below ν(M−C). All the other modes involving displacements of the heavy metal atoms are found in the frequency range [0 cm^{-1}, 300 cm^{-1}].

We now focus on the dependence of the C−O stretching frequency as a function of the adsorption site. Upon atop adsorption on platinum, the predicted ν(C−O) is reduced from 2140 cm^{-1} to 2050 cm^{-1}, corresponding to a red shift $\Delta\nu$(C−O) of −90 cm^{-1}. For comparison, the experimental stretching frequency, as obtained by means of sum-frequency generation (SFG) spectroscopy,[37] decreases from 2170 cm^{-1} to 2070 cm^{-1}, corresponding to $\Delta\nu$(C−O) = −100 cm^{-1}. The frequency shifts are even more marked at high-coordination sites: ν(C−O) is predicted to be 1845 cm^{-1}, 1752 cm^{-1}, and 1743 cm^{-1} at the bridge, hcp, and fcc sites, corresponding to red shifts of up to −397 cm^{-1}. These DFPT stretching frequencies show remarkable agreement with their SFG counterparts: ν(C−O) = 1830 cm^{-1} at the twofold bridge site, ν(C−O) = 1760 cm^{-1} at the threefold hcp and fcc sites, corresponding to a maximum red shift of −410 cm^{-1}. Accurate DFPT frequencies are also obtained for CO adsorbed on platinum−ruthenium bimetallic surfaces. Indeed, the calculated stretching frequencies 1979 cm^{-1} (1 Ru ML) and 1969 cm^{-1} (2 Ru ML) at the atop site compare very closely to the SFG result 1970 cm^{-1}.

In conclusion, all calculated C−O stretching frequencies deviate by less than 2% from the measured ones, irrespective of the adsorption site and nature of the metal surface. The correct prediction of the frequency red shifts allows the direct recognition of CO adsorption sites and confirms that CO preferentially occupies atop sites on platinum−ruthenium bimetallic surfaces. This very close agreement with experiment is made more remarkable by the lack of accuracy of the PBE-GGA adsorption energies. In the remainder of this work, we show how this accuracy can be rationalized in terms of the hybridization of the CO molecular orbitals with the metal bands.

Discussion

Electronic Origins of the Frequency Shifts. The hybridization of the metal d bands with the 2π* lowest unoccupied molecular orbitals (LUMOs) and the 5σ highest occupied molecular orbital (HOMO) plays a predominant role in the adsorption energy of CO on transition metals. According to the Blyholder model,[41] these electronic interactions result in electron donation (i.e., partial depletion of the 5σ orbital) and electron backdonation (i.e., partial filling of the 2π* orbital). It has been shown that the trends of the adsorption energies of CO on transition metal surfaces can be correlated to the amounts of donation and backdonation (Hammer−Morikawa−Nørskov model).[10] Among the suggested solutions to the "CO/Pt(111) puzzle"—e.g., nonequivalent GGA description of different bond orders,[20] incorrect singlet−triplet CO excitation energies,[21] effect of metal semicore polarization[22]—Kresse, Gil, and Sautet have proposed that the inaccuracy of density-functional calculations in determining the most stable adsorption site is due to an overestimation of the interaction between the 2π* orbitals and the metal bands, resulting from an underestimation of the HOMO−LUMO gap.[19] As discussed in the next section, this interpretation recovers the essential features of CO adsorption on transition metals: it identifies the tendency of local and generalized-gradient DFT to delocalize and overhybridize electronic states. Nevertheless, as shown below, the site dependence of the C−O bond length and vibrational frequency is not affected by the LUMO and HOMO hybridizations. In other words, the hybridizations that subtly determine the relative CO adsorption energies do not influence the structural and vibrational predictions.

To establish this fact, we first introduce a spectral force analysis. The main objective of this analysis is to separate and assess the contribution from each CO molecular orbital to the

---

(35) Lu, C.; Lee, I. C.; Masel, R. I.; Wieckowski, A.; Rice, C. *J. Phys. Chem. A* **2002**, *106* (13), 3084−3091.
(36) Ogletree, D. F.; Vanhove, M. A.; Somorjai, G. A. *Surf. Sci.* **1986**, *173* (2−3), 351−365.
(37) Lu, G. Q.; White, J. O.; Wieckowski, A. *Surf. Sci.* **2004**, *564* (1−3), 131−140.
(38) Steininger, H.; Lehwald, S.; Ibach, H. *Surf. Sci.* **1982**, *123* (2−3), 264−282.
(39) Steckel, J. A.; Eichler, A.; Hafner, J. *Phys. Rev. B* **2003**, *68*, 85416−85424.
(40) Baroni, S.; de Gironcoli, S.; Dal Corso, A.; Giannozzi, P. *Reviews Of Modern Physics* **2001**, *73* (2), 515−562.
(41) Blyholder, G. *J. Phys. Chem.* **1964**, *68*, 2772−2777.

force $\boldsymbol{F}$ acting on a given atom. The central quantity we introduce is $\Phi_{I,\chi}(\epsilon)$, the force density of states (FDOS) of the orbital χ, which is defined as the χ-resolved density of states weighted by the wavefunction contribution to the force $\boldsymbol{F}_I$ acting on atom I. To be more explicit, the FDOS of a given CO molecular orbital χ can be expressed as

$$\Phi_{I,\chi}(\epsilon) = \sum_i \boldsymbol{F}_{I,i}\, |\langle\chi|\psi_i\rangle|^2\, \delta(\epsilon - \epsilon_i) \qquad (1)$$

where ψ_i denotes the electronic wavefunction, ϵ_i is the electronic energy, and $\boldsymbol{F}_{I,i} = -f_i \int |\psi_i|^2\ \partial V/\partial \boldsymbol{R}_I$ is the wavefunction contribution to the force $\boldsymbol{F}_I$. (The calculation of the overlap $\langle\chi|\psi_i\rangle$ in the ultrasoft formalism is detailed in the Supporting Information.) It should be noted that, by summing the integrated FDOS $\Phi_{I,\chi}(\epsilon)$ over a complete set of orbitals satisfying orthonormality, one obtains the total electronic force acting on atom I. As a consequence, the FDOS can be quantitatively connected to relevant observables. Additionally, by projecting the force density of states along the normalized atomic displacements $\Delta_I^{(\mathrm{C-O})}$ corresponding to the C−O stretching mode, we obtain the force density of states along the stretching mode $\Phi_\chi^{(\mathrm{C-O})}(\epsilon) = \sum_I \Delta_I^{(\mathrm{C-O})}\, \Phi_{I,\chi}(\epsilon)$, to be heuristically identified as the orbital contribution to the intramolecular force.

The orbital-projected density of states (DOS) $g_\chi(\epsilon) = \sum_i |\langle\chi|\psi_i\rangle|^2\, \delta(\epsilon - \epsilon_i)$ is commonly used to provide an insightful picture of the electronic hybridizations that take place when CO is adsorbed on platinum. Similarly, $\Phi_\chi^{(\mathrm{C-O})}(\epsilon)$ describes the influence of electronic hybridizations on the force along the C−O stretching mode. The projected densities of states $g_\chi(\epsilon)$ and projected force densities of states $\Phi_\chi^{(\mathrm{C-O})}(\epsilon)$ for different adsorption sites are plotted in Figures 1 and 2. A detailed analysis of the orbital-resolved densities of states is given in ref 19. For the purpose of our study, we emphasize the following features. When CO adsorbs on Pt(111), the $4\sigma^*$ and 5σ orbitals hybridize with the metal d_{z^2} band, generating $4\tilde{\sigma}^*$ and $5\tilde{\sigma}$ states with mainly adsorbate character (adopting the terminology of ref 42, the tilde symbol denotes hybrid states). These $4\tilde{\sigma}^*$ and $5\tilde{\sigma}$ states are found in the energy ranges [−12 eV, −9 eV] and [−9 eV, −5 eV] relative to the Fermi level. Above −5 eV, the 5σ orbital and the d_{z^2} band generate a $\tilde{d}_\sigma$ band with predominant metal character. This interaction results in a partial depletion of the 5σ HOMO (electron donation). In addition, the interaction between the 1π and $2\pi^*$ orbitals and the d_{xz} and d_{yz} bands produces $1\tilde{\pi}$ states in the range [−9 eV, −5 eV] and a broad $\tilde{d}_\pi$ band above −5 eV, causing partial occupation of the $2\pi^*$ LUMOs (electron backdonation).[41] The changes in molecular orbital occupations due to CO adsorption are reported in Table 3.

In order to understand how the generation of these hybrid states affects the intramolecular force, we turn to the FDOS (Figure 2). The graphs are plotted according to the convention that bonding states (i.e., opposed to the stretching of the C−O bond) correspond to negative values of $\Phi_\chi^{(\mathrm{C-O})}$. First, we note that the bonding contribution from the 3σ state does not vary with the adsorption site, confirming that the 3σ state retains a strong molecular character. Additionally, we observe that the $5\tilde{\sigma}$ and $1\tilde{\pi}$ states are bonding while the $4\tilde{\sigma}^*$ is antibonding, as expected intuitively. In the energy region above −5 eV, another contribution appears. This contribution corresponds to high-energy wavefunctions located inside the platinum slab, as evidenced by the absence of molecular-orbital force contributions above −5 eV. Nevertheless, due to their metal character, the contribution of these high-energy wavefunctions is mostly cancelled by the positively charged platinum cores. Consequently, the local contribution from the hybrid states of strong molecular character prevails.

(a) Atop DOS

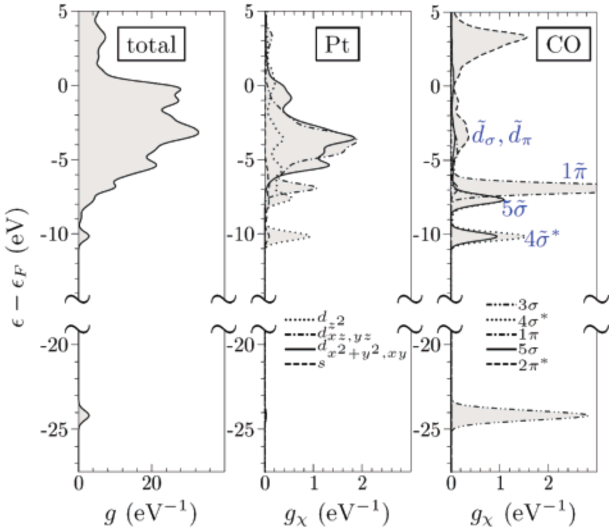

(b) Fcc DOS

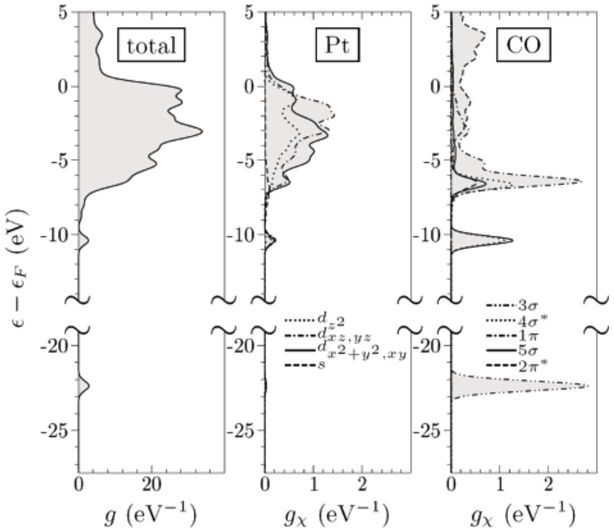

Figure 1. Total density of states, density of states projected on the Pt atomic orbitals, and density of states projected on the CO molecular orbitals for atop and fcc adsorption of CO on Pt(111).

Besides these observations, the main feature of the FDOS graphs is the predominant bonding contribution between −9 eV and −5 eV. At the atop site, the curve displays a sharp negative peak which corresponds mainly to the 1π orbital-resolved contribution $\Phi_{1\pi}^{(\mathrm{C-O})}(\epsilon)$. At the fcc site, both the magnitude and the relative share of the peak are reduced, clearly indicating that the $1\tilde{\pi}$ states have more influence on the change in intramolecular bonding than any of the other hybrid wave-

---

(42) Föhlisch, A.; Nyberg, M.; Hasselström, J.; Karis, O.; Pettersson, L. G. M.; Nilsson, A. *Phys. Rev. Lett.* **2000**, *85* (15), 3309−3312.

(43) Zupan, A.; Burke K.; Ernzerhof M.; Perdew J. P. *J. Chem. Phys.* **1997**,*106* (24), 10184−10193.

(a) Atop FDOS

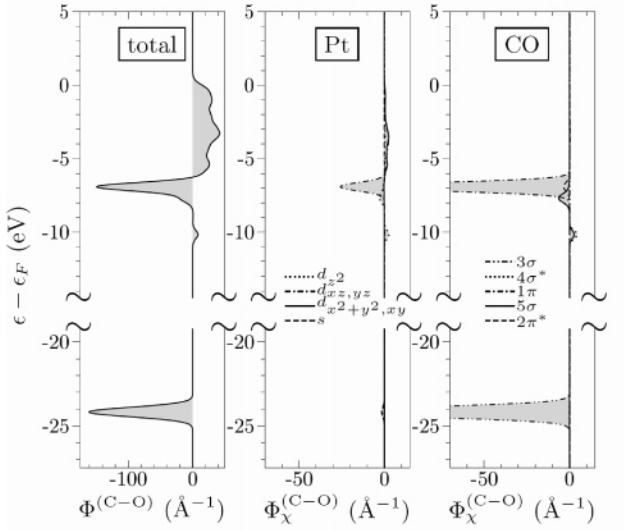

(b) Fcc FDOS

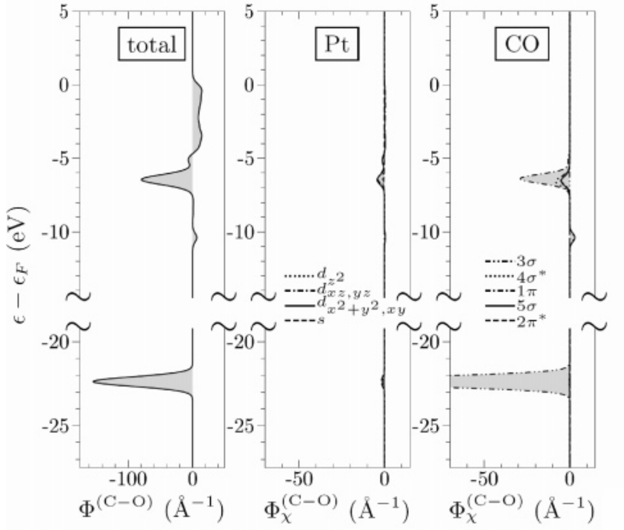

Figure 2. Total force density of states, force density of states projected on the Pt atomic orbitals, and force density of states projected on the CO molecular orbitals for the C−O stretching mode at the atop and fcc adsorption sites for CO on Pt(111).

Table 3. Molecular Occupations and Bond Order for CO in the Gas Phase and CO Adsorbed on Platinum

	gas phase	atop	bridge	hcp	fcc
$f(2\pi_x^*)/2 + f(2\pi_y^*)/2$	0.00	0.25	0.37	0.41	0.41
$f(5\sigma)$	1.00	0.92	0.92	0.92	0.92
$f(1\pi_x)/2 + f(1\pi_y)/2$	1.00	1.00	0.99	0.99	0.99
$f(4\sigma^*)$	1.00	1.00	1.00	1.00	1.00
$f(3\sigma)$	1.00	1.00	1.00	1.00	1.00
bond order	3.00	2.35	2.16	2.09	2.09

functions. The $1\tilde{\pi}$ states maintain a predominant 1π character at the atop site, whereas at high-coordination sites this molecular character is significantly reduced due to a stronger hybridization with the substrate. Therefore, the 1π bonding contribution to the intramolecular force decreases with site coordination. As intramolecular bonding decreases, the C−O bond length increases. The predominance of the 1π bonding contribution is confirmed by the density-distribution analysis initially introduced by Zupan, Burke, Ernzerhof, and Perdew,[43] as discussed in the Supporting Information.

For CO adsorbed on transition metal surfaces, the intramolecular bond length and the intramolecular stretching frequency are strongly correlated. An extensive study of Gajdoš, Eichler, and Hafner[44] showed a linear relationship between d(C−O) and ν(C−O) for CO adsorbed on close-packed transition metals: ν(C−O) shifts down in frequency as d(C−O) increases. Therefore, the increase in C−O bond length at high-coordination sites, which reflects a decrease in 1π bonding contribution, is accompanied by a reduction of the C−O stretching frequency.

In addition to the C−O force analysis, we have calculated the frequency density of states (ωDOS) projected on each molecular orbital. These calculations, which are detailed in the Supporting Information, directly confirm the predominant frequency contribution from the 1π molecular orbitals. It should also be noted that, at variance with the intramolecular FDOS, the analysis of the FDOS projected on the Pt−C stretching mode (cf. Supporting Information) indicates that the Pt−C force is strongly influenced by high-energy metal d bands, thus explaining the lack of accuracy of the ν(Pt−C) predictions.

While the preceding is consistent with the interpretation given in refs 41, 42, and 44, it is important to make one central observation: although the LUMO $2\pi^*$ filling is a reasonable measure of the amount of hybridization between the 1π, $2\pi^*$ orbitals and the metal d_{xz}, d_{yz} bands, filling the $2\pi^*$ orbitals does not directly weaken the bond, as evidenced by the very low values of $\Phi_{2\pi^*}^{(\mathrm{C-O})}(\epsilon)$ in the energy range [−9 eV, −5 eV]. This interpretation helps explain the fact that the CO adsorption energies do not show a well-defined relationship with the C−O stretching frequency.[45,46]

The main conclusion of this section is as follows. At variance with the CO adsorption energies, electron backdonation and electron donation have little direct bearing on the intramolecular forces. Their immediate effect on the molecular bond length and stretching frequency cannot account for the observed shifts. Instead, the changes in bond length and stretching frequency are primarily related to the hybridization of the 1π molecular orbitals. This provides important indications as to why the structural and vibrational properties of CO adsorbed on platinum and platinum−ruthenium surfaces are accurately predicted. The GGA + molecular U study presented in the next part provides additional quantitative evidence in support of this conclusion.

Influence of Donation and Backdonation on the Accuracy of the Frequency Predictions. As mentioned above, the failure of density-functional calculations in predicting CO adsorption energies is traceable to an overhybridization of the CO molecular orbitals with the metal bands.[19,47] To assess the influence of this overhybridization on the accuracy of the calculated adsorption energies, bond lengths, and vibrational properties, we have performed a sensitivity analysis. This analysis consists of controlling and varying the HOMO and LUMO hybridizations, while monitoring the variations of the mentioned observables. To this end, we have used the GGA + molecular U approach introduced by Kresse, Gil, and Sautet.[19] This approach (inspired

---

(44) Gajdoš, M.; Eichler, A.; Hafner, J. *J. Phys. Condens. Matter* **2004**, *16* (8), 1141−1164.
(45) Shubina, T. E.; Koper, M. T. M. *Electrochim. Acta* **2002**, *47* (22−23), 3621−3628.
(46) Han, B. C.; Ceder, G. *Phys. Rev. B* **2006**, *74*, 205418.
(47) Gil, A.; Clotet, A.; Ricart, J. M.; Kresse, G.; García-Hernández, M.; Rösch, N.; Sautet, P. *Surf. Sci.* **2003**, *530* (1−2), 71−86.

by the LDA + U method)[48] consists of adding an orbital-dependent term to the GGA energy functional, thus imposing a penalty on orbital hybridization.

We employ the following GGA + molecular U energy functional:

$$E_{\mathrm{GGA+U}} = E_{\mathrm{GGA}} + \frac{U_{2\pi^*}}{2}\sum_{\sigma} Tr(\mathbf{f}_{2\pi^*,\sigma}(\mathbf{I} - \mathbf{f}_{2\pi^*,\sigma})) + \frac{U_{5\sigma}}{2}\sum_{\sigma} f_{5\sigma,\sigma}(1 - f_{5\sigma,\sigma}) \quad (2)$$

where $f_{5\sigma,\sigma}$ is the occupation of the 5σ orbital of spin σ and $\mathbf{f}_{2\pi^*,\sigma}$ is the occupation matrix associated with the $2\pi_x$* and $2\pi_y$* orbitals of spin σ. The parameters $U_{2\pi}$* and $U_{5\sigma}$ penalize noninteger occupations of the 2π* and 5σ orbitals: $U_{2\pi}$* reduces 2π* backdonation while $U_{5\sigma}$ reduces 5σ donation, as illustrated in Figure 3. The parameters $U_{2\pi^*}$ and $U_{5\sigma}$ can also be interpreted as shifting the effective single-electron energies. Heuristically, U_χ modifies the single-electron energy ϵ_χ by an amount $\Delta\epsilon_\chi \approx U_\chi(^1/_2 - f_\chi)$. Thus, $U_{2\pi^*}$ increases the 2π* energies, whereas $U_{5\sigma}$ decreases the 5σ energy, causing the HOMO−LUMO gap to increase. Changes in single-electron energies as a function of $U_{2\pi^*}$ and $U_{5\sigma}$ are reported in the Supporting Information.

The present functional differs slightly from that introduced by Kresse, Gil, and Sautet. The GGA + molecular U energy in (eq 2), whose expression is based on the matrix formulation introduced by Cococcioni and de Gironcoli,[49] is invariant with respect to the choice of the *x*- and *y*-axes. In other words, an arbitrary rotation of the molecular orbitals does not affect the GGA + molecular U energy. Additionally, the functional allows the freedom to vary both the amount of electron backdonation and that of electron donation. The necessity of simultaneously varying backdonation and donation will be discussed later.

Although a molecular U term is admittedly a simplified energy correction, it reproduces the essential features of the energetics of CO adsorption.[19] The cluster calculations of Gil et al., based on the B3LYP hybrid functional,[50] confirm that the inaccuracy of the GGA energies can be ascribed to an overhybridization of the 2π* molecular orbitals.[47] This conclusion is supported by the recent periodic-slab B3LYP calculations of Neef and Doll.[23,24] Moreover, experimental studies indicate that the adsorption energy of CO on platinum shows a linear dependence with respect to the energy of the center of the metal d bands,[35] in agreement with the theoretical model developed by Hammer, Morikawa, and Nørskov.[10] However, the coefficient of proportionality is overestimated within density-functional calculations, indicating that the interaction between the 2π* orbitals and the metal d bands is excessive.

We thus proceeded to calculate the energetic, structural, and vibrational properties for CO adsorbed on platinum. Stretching frequencies are now obtained by diagonalizing the two-by-two dynamical matrix associated with off-equilibrium displacements of the carbon and oxygen atoms in the direction normal to the surface. Due to the large atomic mass of platinum, the resulting stretching frequencies deviate by less than 1 cm^{-1} from the full DFPT phonon frequencies.

(a) Atop DOS vs. $U_{2\pi^*}$

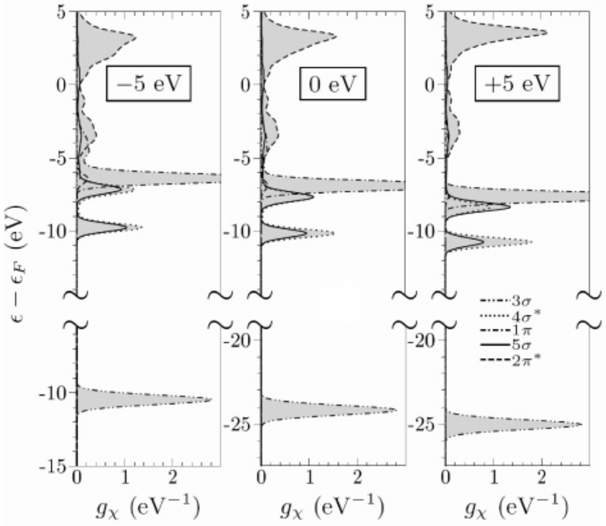

(b) Atop DOS vs. $U_{5\sigma}$

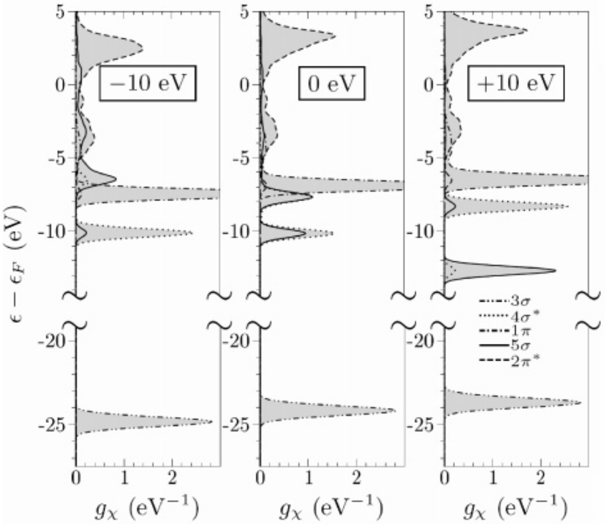

Figure 3. Density of states projected on the CO molecular orbitals as a function of $U_{2\pi^*}$ and $U_{5\sigma}$ controlling the hybridization of the LUMO and HOMO orbitals for atop adsorption of CO on Pt(111).

The results of the calculations are presented in Figure 4 and in the Supporting Information. As expected, adsorption energies decrease with increasing penalization on the hybridizations of the HOMO and LUMOs (cf. Supporting Information). Consequently, both donation and backdonation favor CO adsorption, in agreement with ref 19. Moreover, we observe that electron backdonation tends to decrease the relative adsorption energy E_{ads}(atop) − E_{ads}(fcc), confirming that 2π* backdonation favors CO adsorption at high-coordination sites, as demonstrated by Anderson and Awad.[51] Additionally, the effect of $U_{5\sigma}$ on the relative binding energy is much weaker than that of $U_{2\pi}$*. This result supports the hypothesis that the failure of density-functional calculations in predicting the most stable adsorption site is principally related to an overestimation of 2π* backdonation.[17−19]

---

(48) Anisimov, V. I.; Aryasetiawan, F.; Lichtenstein, A. I. *J. Phys. Condens. Matter* **1997**, *9* (4), 767−808.
(49) Cococcioni, M.; de Gironcoli, S. *Phys. Rev. B* **2005**, *71*, 35105−35120.
(50) Becke, A. D. *J. Chem. Phys.* **1993**, 98 (7), 5648−5652.
(51) Anderson, A. B.; Awad, M. K. *J. Am. Chem. Soc.* **1985**, *107* (26), 7854−7857.
(52) Baroni, S.; Dal Corso, A.; de Gironcoli, S.; Giannozzi, P.; Cavazzoni, C.; Ballabio, G.; Scandolo, S.; Chiarotti, G.; Focher, P.; Pasquarello, A.; Laasonen, K.; Trave, A.; Car, R.; Marzari, N.; Kokalj, A. *Quantum-Espresso* (http://www.quantum-espresso.org).

(a) $E_{ads}(\mathrm{atop}) - E_{ads}(\mathrm{fcc})$ (eV)

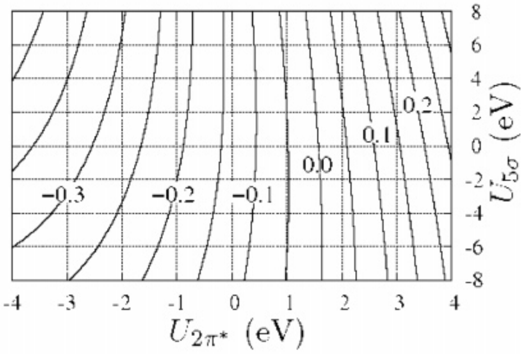

(b) $\nu(\mathrm{C-O})(\mathrm{atop})$ (cm^{-1})

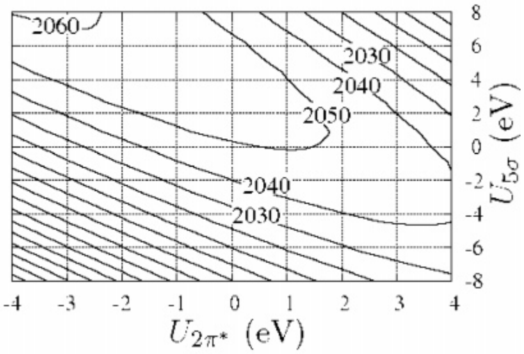

(c) $\nu(\mathrm{C-O})(\mathrm{fcc})$ (cm^{-1})

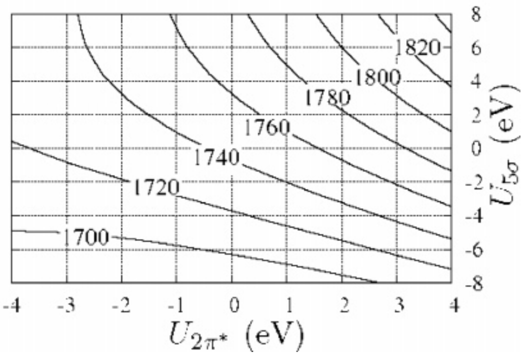

Figure 4. Adsorption energy difference and C−O stretching frequency as functions of $U_{2\pi^*}$ and $U_{5\sigma}$ controlling the hybridization of the LUMO and HOMO orbitals for atop and fcc adsorption of CO on Pt(111).

Considering now the structural and vibrational properties, we observe more complex $U_{5\sigma}$- and $U_{2\pi^*}$-dependencies. The effect of electron donation must clearly be taken into account when analyzing the sensitivity of the calculated stretching frequencies. Note that the invariance of the stretching frequency with respect to $U_{2\pi^*}$ for CO adsorbed at the atop site, as already observed in ref 17 for copper surfaces, can be explained by the fact that the $U_{2\pi^*}$-axis is tangent to the contour line $\nu(\mathrm{C-O}) = 2050$ cm^{-1}. Despite this fact, the dependence of $\nu(\mathrm{C-O})(\mathrm{atop})$ with respect to $U_{5\sigma}$ is appreciable, supporting the idea that $2\pi^*$ backdonation alone does not control the site dependence of the C−O stretching frequency.

To conclude this section, we report the results of our sensitivity analysis (Figure 5). Large ranges for $U_{2\pi^*}$ and $U_{5\sigma}$ are selected: 0 eV $< U_{2\pi^*} <$ 5 eV and −10 eV $< U_{5\sigma} <$ 10 eV. Note that the parameter $U_{2\pi^*}$ is kept positive since the GGA + molecular U calculations clearly indicate that $2\pi^*$ backdonation is overestimated. We emphasize that these energy ranges correspond to large shifts in the single-electron energies (up to $\Delta\epsilon_{2\pi^*} = 1$ eV and $|\Delta\epsilon_{5\sigma}| = 4$ eV) and to large variations of the adsorption energies (up to $|\Delta E_{ads}| = 1.5$ eV). Thus, the relative variations of the adsorption energies are comparable to their absolute values. Despite the sizable variations of the adsorption energies, we observe little variations of the bond lengths and stretching frequencies:

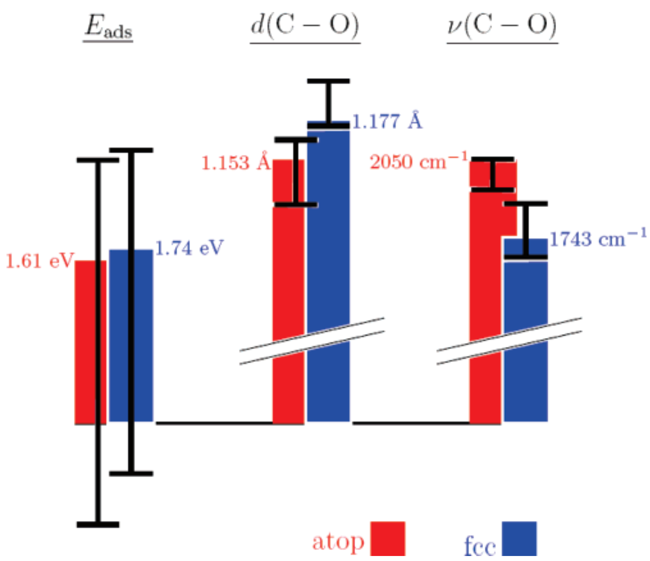

Figure 5. Ranges of variation (indicated by black error bars) of the adsorption energy, bond length, and stretching frequency of CO on Pt(111) for a very broad range of hybridizations (0 eV $< U_{2\pi^*} <$ 5 eV and −10 eV $< U_{5\sigma} <$ 10 eV).

$$1.127\ \text{Å} < d(\mathrm{C-O})(\mathrm{atop}) < 1.165\ \text{Å}$$

$$1.173\ \text{Å} < d(\mathrm{C-O})(\mathrm{fcc}) < 1.199\ \text{Å}$$

$$1933\ \mathrm{cm}^{-1} < \nu(\mathrm{C-O})(\mathrm{atop}) < 2055\ \mathrm{cm}^{-1}$$

$$1666\ \mathrm{cm}^{-1} < \nu(\mathrm{C-O})(\mathrm{fcc}) < 1878\ \mathrm{cm}^{-1}$$

These small variations account for the remarkable accuracy of the bond lengths and stretching frequencies calculated within PBE-GGA. In particular, they justify the correct ordering of the C−O stretching frequencies despite important qualitative errors in predicting the relative CO adsorption energies. These results provide strong support to the conclusion of the preceding section: the variations of $d(\mathrm{C-O})$ and $\nu(\mathrm{C-O})$ are not directly due to electron donation and backdonation, but rather to the hybridization of the 1π orbitals.

Conclusion

This study has evidenced that the PBE-GGA predictions for the stretching frequencies of CO adsorbed on platinum are in excellent agreement with SFG experiments despite the well-known failure of local and generalized-gradient calculations in predicting the most stable adsorption site. Similar agreement is obtained for CO adsorbed on platinum−ruthenium bimetallic surfaces, allowing the direct recognition of CO adsorption sites.

Our orbital-resolved force analysis has demonstrated that the variations of bond length and stretching frequency as a function of the CO adsorption site are principally due to the 1π hybridization instead of the $2\pi^*$ and 5σ hybridizations. Using the GGA + molecular U approach, we have performed a sensitivity analysis to quantify the influence of the $2\pi^*$ and 5σ hybridizations on the structural and vibrational properties for CO on platinum. The effect of $2\pi^*$ backdonation has been shown to be small and comparable to that of 5σ donation, contradicting the widespread idea that backdonation controls the frequency shifts.

These results explain the remarkable accuracy of the PBE-GGA frequency predictions despite errors in the hybridizations of the $2\pi^*$ and 5σ orbitals. Furthermore, they suggest a promising way to connect density-functional calculations with experiments in some of the most problematic cases of molecular adsorption on transition metals.

Acknowledgment. The calculations in this work have been performed using the Quantum-Espresso package.[52] The authors acknowledge support from the MURI Grant DAAD 19-03-1-0169. Computational facilities have been provided through NSF-DMR-0414849 and PNNL-EMSL-UP-9597. Ismaila Dabo thanks the École Nationale des Ponts et Chaussées (France) and the Martin Family Society of Fellows for Sustainability for their help and support. Valuable discussions with Matteo Cococcioni, Cody Friesen, Brandon Wood, and Fabien Sorin are gratefully acknowledged.

Supporting Information Available: Results of the ωDOS frequency analysis, details about the calculation of wavefunction overlaps with ultrasoft pseudopotentials, presentation of the GGA + molecular U FDOS method, results of the Zupan−Burke−Ernzerhof−Perdew density-distribution analysis, details on the pseudopotentials, and additional data. This material is available free of charge via the Internet at http://pubs.acs.org.

JA067944U